Stochastic Distribution System Operation Considering Voltage Regulation Risks in the Presence of PV Generation

Yashodhan P. Agalgaonkar, *Student Member, IEEE*, Bikash C. Pal, *Fellow, IEEE*, and Rabih A. Jabr, *Senior Member, IEEE*

***Abstract*—Variable over voltage, excessive tap counts, and voltage regulator (VR) *runaway* condition are major operational challenges in distribution network while accommodating generation from photovoltaics (PVs). The conventional approach to achieve voltage control based on offline simulation for voltage set point calculation does not consider forecast errors. In this work, a stochastic optimal voltage control strategy is proposed while considering load and irradiance forecast errors. Stochastic operational risks such as overvoltage and VR runaway are defined through a chance constrained optimization (CCO) problem. This classical formulation to mitigate runaway is further improved by introducing a stochastic index called the *Tap Tail Expectation*. Operational objectives such as power losses and excessive tap count minimization are considered in the formulation. A sampling approach is proposed to solve the CCO. Along with other voltage control devices, the PV inverter voltage support features are coordinated. The simulation study is performed using a realistic distribution system model and practically measured irradiance to demonstrate the effectiveness of the proposed technique. The proposed approach is a useful operational procedure for distribution system operators. The approach can minimize feeder power losses, avoid voltage violations, and alleviate VR runaway.**

***Index Terms*—Distribution voltage control, photovoltaic (PV) forecast errors, voltage regulator (VR) runaway.**

I. Introduction

THE RENEWABLE portfolio initiatives in various countries are acting as a stimulus for the growth of grid connected renewable generation sources such as photovoltaics (PVs). The global cumulative PV generation capacity is expected to reach 200 GW by 2017 [1]. PV systems are mostly integrated at the medium-voltage (MV) and low-voltage (LV) distribution system levels. For instance, in Germany, where the installed peak capacity is 31 GWp, around 95% of PV generation is connected to the LV and MV distribution grid [2].

One of the major operational challenges faced by distribution network operators (DNOs) is voltage rise due to the integration of PV [3]. During unity power factor (pf) operation of PV, the DNOs control overvoltage by active power curtailment [4]. The reactive power support functionality from the PV inverter interface also can be utilized to control overvoltage [5]–[7]. This functionality can be in the form of autonomous settings, such as variation in power factor as active power varies [pf(P) setting] or variation in reactive as voltage varies [Q(U) setting]. Unlike autonomous settings, the voltage control setpoints can also be communicated to the PV inverter through remote control [8], [9]. Besides PV inverter voltage control features, classical equipments such as the on load tap changer (OLTC) and the voltage regulator (VR) are also utilized to manage the voltage in the network.

The challenge of voltage control is further intensified by the fact that PV generation has an impact on the action of OLTC and VR. The variable voltage rise due to the PV generation results in an increase of OLTC and VR tap counts and hence leads to an increased maintenance frequency of these devices. VR operating at its limit due to *reverse power tap changer runaway* is also another critical problem [10]. Under runaway scenario, VR fails to control voltage at the regulated bus and reaches lowest or highest tap limit. Runaway happens due to the interaction between VR control settings and PV reactive power support. It also depends upon several other factors such as PV capacity, load and irradiance values, voltage setpoints of devices, and distribution feeder topology. Clearly, the operation of VR at its limit can result in extreme low or extreme high voltage on the feeder. Furthermore, during the runaway operation, the controllability of VR is lost. A detailed assessment of the effect of PV on VR runaway is presented in [11]. Some of these challenges are addressed through supervisory control [12]–[14]. However, all these efforts ignored the errors associated with the load and PV generation forecasting [15], [16].

Since there is an element of randomness associated with forecast errors, it is necessary to deal with this problem via stochastic approaches. The probabilistic load flow (PLF) analysis to evaluate the impact of PV generation is proposed in [17]. Furthermore, probabilistic optimal power dispatch considering uncertainty in the presence of PV generation is formulated in [18]. The stochastic nature of output from Distributed Generator (DG) is characterized through the

Manuscript received September 11, 2014; revised April 13, 2015; accepted May 12, 2015. Date of publication June 11, 2015; date of current version September 16, 2015. This work was supported in part by U.K.–India initiative in solar energy through a project "Stability and Performance of Photovoltaic (STAPP)" funded by Research Councils U.K. (RCUK) Energy Programme in U.K. (Contract EP/H040331/1) and in part by the Department of Science and Technology (DST) in India. Paper no. TSTE-00467-2014.

Y. P. Agalgaonkar was with the Department of Electrical and Electronic Engineering, Imperial College, London SW7 2AZ, U.K. He is now with Pacific Northwest National Laboratory, Richland, WA 99354 USA (e-mail: yashodhan.imperial@gmail.com).

B. C. Pal is with the Department of Electrical and Electronic Engineering, Imperial College, London SW7 2AZ, U.K. (e-mail: b.pal@imperial.ac.uk).

R. A. Jabr is with the Department of Electrical and Computer Engineering, American University of Beirut, Beirut 1107 2020, Lebanon (e-mail: rabih.jabr@aub.edu.lb).

Digital Object Identifier 10.1109/TSTE.2015.2433794

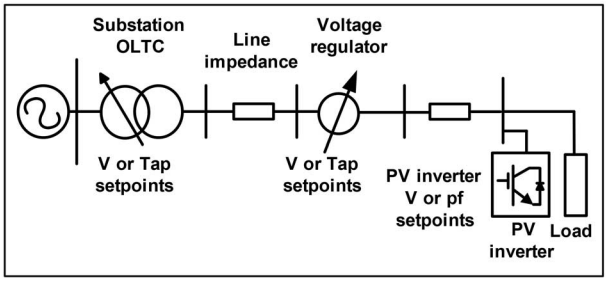

Fig. 1. Voltage control of a radial distribution feeder [10].

probability distribution function (pdf) and subsequently the expectation of power loss is formulated as an objective function for minimization [19]. However, the formulation in [19] did not include different constraint violations in a stochastic sense. A constrained PLF (CPLF) that examines constraint violations while carrying out reactive power coordination is proposed in [20]. The stochastic predictions of the power flows and voltage levels in distribution systems having renewable energy generation is carried out in [21]. Analytical PLF-based chance constrained optimization (CCO) is employed in [22] to achieve reactive power coordination. Monte Carlo simulation (MCS)-based stochastic optimization to calculate renewable energy pf setpoints is proposed in [23]. The available literature does not, however, consider the VR runaway in system operation, including the forecast errors. This motivated us to pursue our research effort to propose a stochastic framework that minimizes the risk of VR runaway. In this work, a stochastic distribution voltage control strategy is proposed. This paper is structured as follows. In Section II, stochastic operation considering VR runaway is formulated as a classical CCO problem. A CCO solution strategy is proposed in Section III. Section IV defines an appropriate stochastic index, which further minimizes the risk of VR runaway. Section V presents a case study to demonstrate the effectiveness of the proposed approach. Section VI concludes this paper.

II. Distribution Voltage Control

The stochastic operation of the radial feeder shown in Fig. 1 is under consideration. In order to achieve an optimal operation, DNOs should consider different objectives and risks. A CCO-based problem is formulated to achieve these objectives in the presence of PV generation and load forecast errors. The optimization design (or control) variables are the OLTC voltage setpoints and the PV inverter voltage setpoints. The distribution system line data, load data, and PV/load forecast errors are given problem parameters. Bus voltages and line currents in the system are dependent variables. The problem is mathematically formulated as follows.

A. Optimization Objective

DNOs wish to operate distribution feeders such that the losses are minimum. The expected value of power loss should be minimized in order to account for randomness in forecasting errors, i.e.,

$$\text{Minimize } E(P_{\text{loss}}) \tag{1}$$

where $E(P_{\text{loss}})$ represents the expected value of power losses in the time horizon under consideration.

B. Optimization Constraints

1) *Bus voltage*: The primary objective of any feeder operational strategy is to maintain acceptable bus voltages. When the forecast errors are considered, the bus voltage violation risk needs to be accounted for. Variance minimization can be utilized if DNOs insist on maintaining a flat voltage profile. Generally, the bus voltages are required to stay within the specific band $(0.95-1.05$ p.u.) [13], [24]. Therefore, minimizing the probability of violation of this band results in an acceptable voltage profile. The voltage violation probability should be below the tolerance prescribed by a DNO. $\Pr(V \leq V_{\text{limit}}^{\text{up}}) \geq \alpha_V^{\text{up}}$ is defined as a constraint for the upper limit of the voltage

$$\Pr(V > V_{\text{limit}}^{\text{up}}) \leq 1 - \alpha_V^{\text{up}}. \tag{2}$$

Similarly, for the lower limit of the voltage

$$\Pr(V < V_{\text{limit}}^{\text{low}}) \leq 1 - \alpha_V^{\text{low}}. \tag{3}$$

In (2) and (3), $V_{\text{limit}}^{\text{up}}$, $V_{\text{limit}}^{\text{low}}$, α_V^{low}, and α_V^{up} are design parameters. These can be changed to suit the requirements of the DNO. $1 - \alpha_V^{\text{up}}$ and $1 - \alpha_V^{\text{low}}$ indicate voltage violation probabilities. Typically, a bus voltage violation is restricted below 5% as per the the European standard EN50160.

2) *Power balance*: In a practical distribution system, power flow equality constraints must be satisfied for each load and irradiance scenario under consideration. This is achieved by a set of nodal current injection equations formulated in rectangular coordinates. The detailed modeling of system components such as lines and transformers in the current injection-based formulation is as per [25] and [26].

3) *Feeder current*: The feeder current thermal capacity needs to be considered in the following manner:

$$\Pr(I_{\text{feed}} > I_{\text{feed}}^{\text{limit}}) \leq 1 - \alpha_I^{\text{feed}}. \tag{4}$$

Typically, α_I^{feed} can be 95% [23]. $I_{\text{feed}}^{\text{limit}}$ changes from season to season. α_I^{feed} and $I_{\text{feed}}^{\text{limit}}$ can be adjusted as per the operator needs.

4) *PV generation*: From a PV generation owner's perspective, revenue should be maximized. This necessitates that the injected active power should always satisfy the maximum power point tracker (MPPT) criterion. However, in order to manage an overvoltage, active power curtailment is unavoidable in some cases. The situation can be best addressed by keeping the expectation of active power curtailment below a specific limit ($\epsilon_{\text{pcurtail}}$) i.e.,

$$E(P_{\text{curtail}}) \leq \epsilon_{\text{pcurtail.}} \tag{5}$$

This active power curtailment is typically 30% in Germany [8]. However, one should aim for less active

power curtailment. $\epsilon_{\mathrm{pcurtail}}$ is a tolerance, which can be adjusted by the DNO. Furthermore, the PV generation reactive power support is limited by its inverter apparent power rating.

5) *OLTC and VR*: The OLTCs and VRs are primarily responsible for feeder voltage control. Details of the technical operation of the OLTC mechanism can be found in [27]. An operator typically specifies the particular voltage setpoint to control the voltage of a regulated bus. One of the major challenges in the presence of PV generation is the excessive number of tap operations required to contain overvoltage. Although there are some new power-electronic OLTCs that can withstand too many tap changes, still many practical feeders operate with conventional electromechanical OLTCs. For these conventional OLTCs and VRs, excessive tap operations reduce the operating life significantly thus requiring an increased number of maintenances. Therefore, voltage control should be achieved with a minimum number of tap operations

$$E(\mathrm{Tap}_{\mathrm{counts}}) \leq \epsilon_{\mathrm{Tapcounts}} \tag{6}$$

where $E(\mathrm{Tap}_{\mathrm{counts}})$ represents the expected value of tap counts in the time horizon under consideration. $\epsilon_{\mathrm{Tapcounts}}$ defines the maximum permissible tap counts.

Another challenge thrown by PV is VR runaway. A VR runaway occurs due to the interactions between VR and PV generation control settings. There are several operational scenarios when a VR runaway is possible. Detailed description of the runaway phenomenon can be found in [11]. This phenomenon results in the operation of the VR either at the lowest or at the highest tap position. The VR runaway also results in the extreme low or high voltage on a feeder. Hence, avoiding operation of a VR at the extreme tap position is essential. A tap violation probability for VR is defined to mitigate the VR runaway, according to the following constraints:

$$\begin{aligned} \Pr(\mathrm{Tap} > \mathrm{Tap}^{\mathrm{up}}_{\mathrm{limit}}) &\leq 1 - \alpha^{\mathrm{up}}_{\mathrm{Tap}} \\ \Pr(\mathrm{Tap} < \mathrm{Tap}^{\mathrm{low}}_{\mathrm{limit}}) &\leq 1 - \alpha^{\mathrm{low}}_{\mathrm{Tap}}. \end{aligned} \tag{7}$$

The regions beyond the Tap values $\mathrm{Tap}^{\mathrm{low}}_{\mathrm{limit}}$ and $\mathrm{Tap}^{\mathrm{up}}_{\mathrm{limit}}$ are denoted as the *nonpreferred zones*. DNOs can mitigate the runaway and maintain VR control margins by specifying $\mathrm{Tap}^{\mathrm{low}}_{\mathrm{limit}}$, $\mathrm{Tap}^{\mathrm{up}}_{\mathrm{limit}}$, $\alpha^{\mathrm{up}}_{\mathrm{Tap}}$, and $\alpha^{\mathrm{low}}_{\mathrm{Tap}}$. The problem is solved through coordination among various reactive power devices in the network. The following section details the solution of this CCO problem.

III. CCO Solution Strategy

Fig. 2 details the general flowchart of the proposed algorithm. The proposed CCO solution algorithm has three major routines: 1) sample selection; 2) set point calculation; and 3) set point validation. These three subroutines are described below.

Step 1) *Sample selection*: Both load and PV generation forecasting errors are considered in the particular time horizon. The time horizon can be day ahead or hour ahead based on the operators' choice. In order to solve the CCO problem, N independent identically distributed sample scenarios are selected. Let $F^{\mathrm{lim}}_{\mathrm{x}}$ denote the probability for which constraints defined for decision variable vector $\boldsymbol{x}$ are violated. Let us also denote α as the acceptable probability level for which constraints are not violated. Hence, the acceptable constraint violation probability β is calculated as $\beta = 1 - \alpha$. A β-level robustly feasible optimization solution will satisfy $F^{\mathrm{lim}}_{\mathrm{x}} \leq \beta$. The number of N different samples to obtain a robust solution are selected as

$$N \geq \frac{n}{\beta\gamma} - 1. \tag{8}$$

where n represents the number of decision variables. If the program is convex, then the extraction of these N samples ensures that the obtained optimization solution is β-level robustly feasible with a probability no smaller than $1 - \gamma$ [28]. Given that convexity does not hold for the problem under study, setpoint validation is, therefore, employed in Step 3). Fig. 3 details the general flowchart for this step.

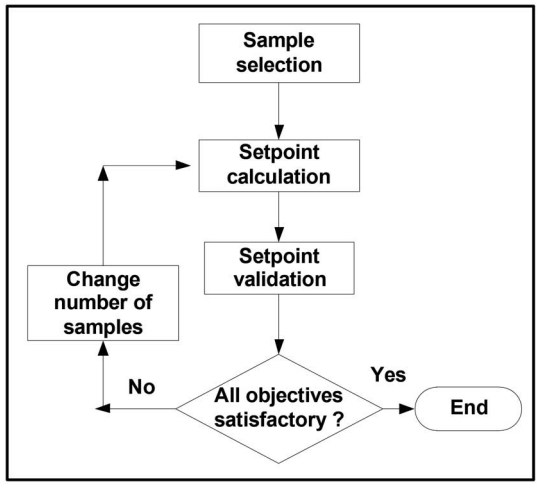

Fig. 2. CCO solution strategy general flowchart.

Step 2) *Setpoint calculation*: This subroutine calculates the setpoints of voltage control devices utilizing the N samples chosen in Step 1). The optimization problem proposed in Section II is a NP-hard problem. It involves nonlinear constraints and discrete variables together with multiple operating scenarios. The problem is not simply solved for each load and PV power sample, because the solution of the problem for every sample will lead to N different PV and OLTC voltage setpoints. In a practical setting, the network operator is interested in a unique PV and OLTC setpoints, which will minimize the risk of runaway and voltage violation over a given time horizon. The solution technique used here is based on an oriented discrete descent method, which is a method adopted by the industry for handling discrete variables in deterministic constraints [29]. This paper extends the use of

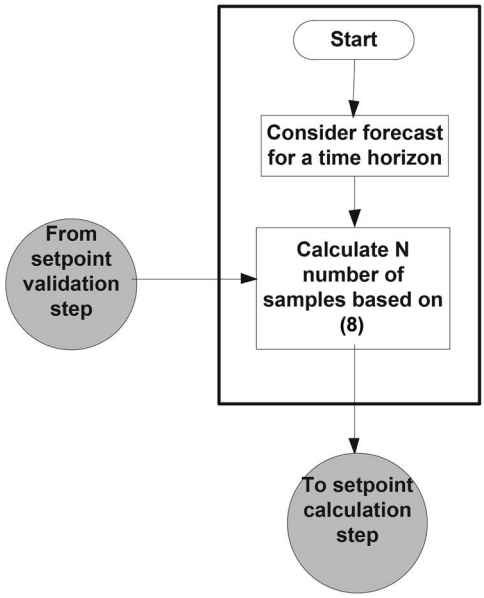

Fig. 3. CCO solution strategy sample selection.

the oriented discrete descent method for handling discrete variables in chance constraints. For N-samples under consideration, the distribution load flow is run for each sample ensuring the power flow equality constraints. Now after N power flow calculations, the expected values of power losses and various constraint violation probabilities can be calculated. If these values are not acceptable to the operator, then the PV inverter setpoint or OLTC voltage setpoint is altered by the oriented discrete descent method. First, the objective function is calculated for some initially assumed values of the control variables (PV inverter setpoint or OLTC voltage setpoint). The control variables are then altered in discrete steps along all possible search directions.

Again for all the new control variable values, the corresponding new values of the objective functions are computed. The partial derivatives of the objective function with respect to all control variables are calculated. The partial derivatives are computed using the differences of the objective function divided by the corresponding variation in the setpoints. The control setpoint with the highest partial derivative is the best candidate to minimize the objective. Only the setpoint that corresponds to the highest value of the partial derivative is altered to minimize the objective. This procedure is repeated until satisfactory variables for the objective function and constraint violation probabilities are obtained. Fig. 4 details the general flowchart for this step.

Step 3) *Setpoint validation*: The calculated setpoints in Step 2) are valid for N samples and they offer a β-level robustly feasible solution [with a minimum probability of (1-gamma)] only if the program is convex. The setpoint validation is carried out to overcome this issue. Expression (8) in the Step 1) is utilized only to give an initial estimate of the number of N minimum samples that must be considered if a certain violation probability is desired. It should be emphasized that because the problem is nonconvex, the set-points need to be validated via MCS, i.e., the solution obtained in Steps 1) and 2) cannot be considered as the final solution. The calculated setpoints are validated by choosing M samples such that $M \gg N$. MCS using the calculated setpoints is run. The objective function and constraint violation probabilities are checked for these M samples. The initially chosen N samples are increased if the validation results are not satisfactory. Upon increasing these N samples, Steps 2) and 3) of the algorithm are rerun until a satisfactory result is obtained. The violation probability β or the confidence parameter γ in (8) can be reduced to increase the value of N. Fig. 5 details the general flowchart for this step.

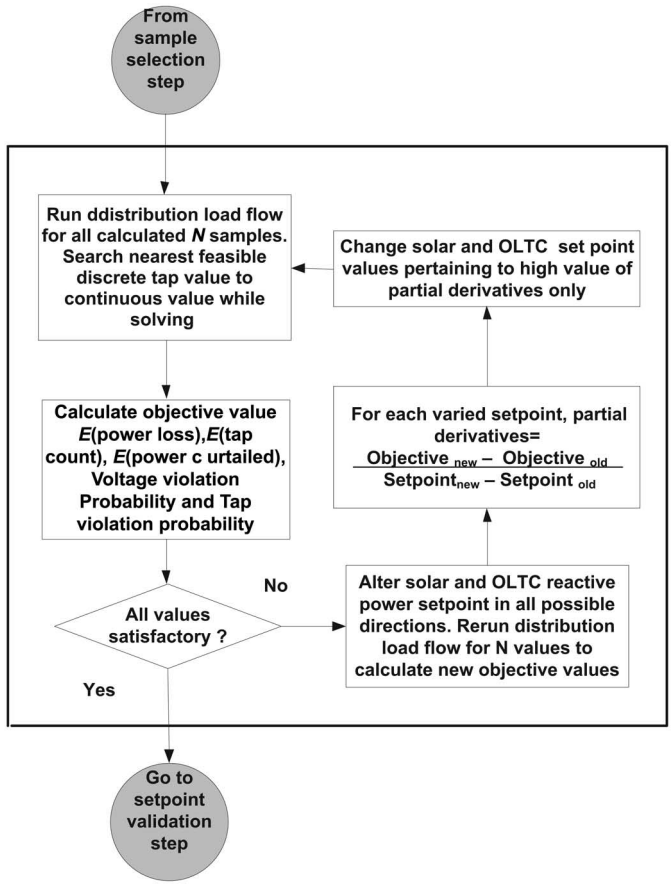

Fig. 4. CCO solution strategy setpoint calculate.

As mentioned in the sample selection subroutine, the setpoints can be calculated for any time horizon. The operational strategy proposed here is subdivided into two distinct time horizons to minimize the impact of forecasting errors. First, a day-ahead time horizon is considered. In this stage, the voltage setpoints of the OLTC and PV generation are calculated. The second stage is particularly useful when a day-ahead PV forecast accuracy is lower. In the second stage, a shorter forecast horizon of 1 h is considered. Hour-ahead PV forecast errors are

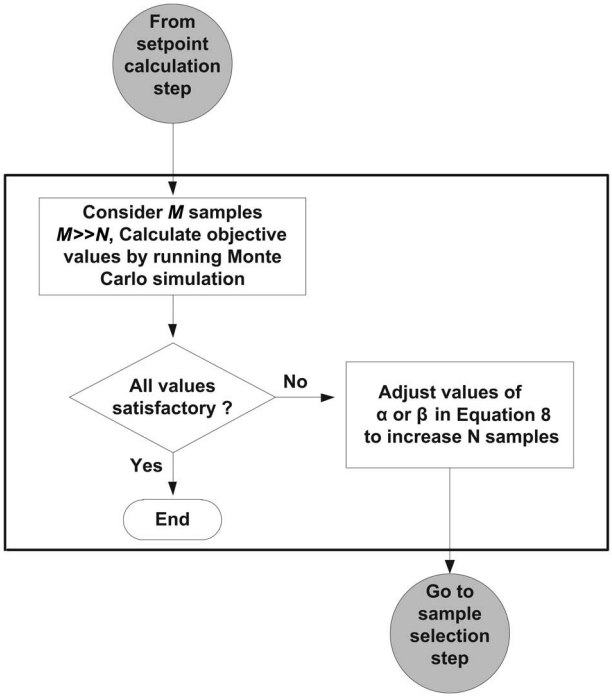

Fig. 5. CCO solution strategy setpoint validation step.

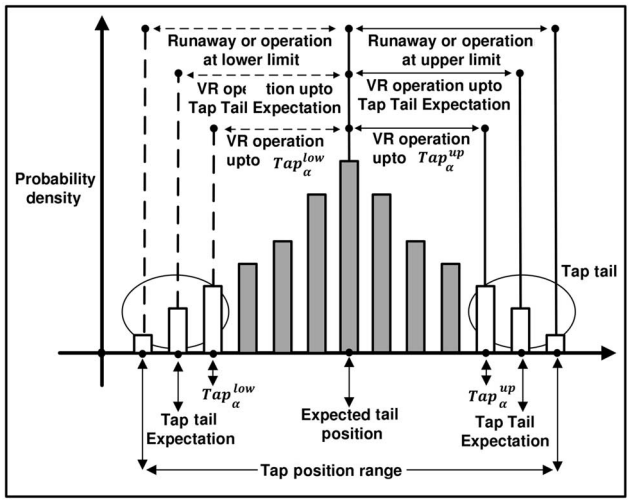

Fig. 6. *Tap Tail Expectation* to mitigate VR runaway.

lower as compared to day-ahead forecast errors [15]. The readjustment of voltage setpoints is done considering an hour-ahead forecast. While readjusting, the OLTC setpoints calculated from the first stage remain the same. Only the PV generation setpoints are readjusted. Communicating voltage setpoints to OLTC and PV generation helps to achieve an efficient operation of a distribution system and mitigates the autonomous VR runaway risk.

IV. Tap Tail Expectation

The CCO discussed above considers VR *runaway* risks by enforcing constraints on tap violation probability. The proposed CCO implementation calculates OLTC and PV inverter setpoints such that the tap positions near the end of the VR tap limit (± 16) lie in the tail region of the VR tap pdf. The parameters such as $\mathrm{Tap}^{\mathrm{up}}_{\mathrm{limit}}$, $\mathrm{Tap}^{\mathrm{low}}_{\mathrm{limit}}$, and α defined in (7) are designed to achieve this. However, its major disadvantage is due to the fact that CCO does not give information about the scenarios where Tap values are beyond $\mathrm{Tap}^{\mathrm{up}}_{\mathrm{limit}}$ or $\mathrm{Tap}^{\mathrm{low}}_{\mathrm{limit}}$. For instance, consider that the permissible probability of the tap value being beyond $+11$ is 5%. Then in 95% of cases, it is ensured that a VR will not operate beyond the value $+11$. But the disadvantage is that in 5% of the cases there is no operational control at which tap position VR will operate. In 5% of cases, a VR can be operating even at $+16$, which indicates the runaway or lack of VR operational margin.

In order to mitigate this limitation, the *Tap Tail Expectation* index is defined. Fig. 6 demonstrates the concept of *Tap Tail Expectation* for VR runaway. The mathematical definition of this risk measure is detailed as follows.

Let $F^{\mathrm{up}}_{\mathrm{Tap}}(z) = \Pr\{\mathrm{Tap} \le z\}$ define the cumulative distribution function (cdf) of a variable Tap. The $\mathrm{Tap}^{\mathrm{up}}_{\alpha}$ with a confidence level $\alpha \in [0,1]$ is defined as

$$\mathrm{Tap}^{\mathrm{up}}_{\alpha} = \min\{z | F^{\mathrm{up}}_{\mathrm{Tap}}(z) \ge \alpha\}. \tag{9}$$

$\mathrm{Tap}^{\mathrm{up}}_{\alpha}$ is a lower α-percentile of the random variable Tap. For example, suppose that the desired value of probability α is 95%. This indicates that for only 5% of instances, Tap attains a value greater than or equal to $\mathrm{Tap}^{\mathrm{up}}_{\alpha}$. Similarly, for the lower limit of the VR, if the cdf is defined as $F^{\mathrm{low}}_{\mathrm{Tap}}(z) = \Pr\{\mathrm{Tap} \ge z\}$ then

$$\mathrm{Tap}^{\mathrm{low}}_{\alpha} = \max\{z | F^{\mathrm{low}}_{\mathrm{Tap}}(z) \ge \alpha\}. \tag{10}$$

In other words, $\mathrm{Tap}^{\mathrm{up}}_{\alpha}$ should be less than $\mathrm{Tap}^{\mathrm{up}}_{\mathrm{limit}}$. Thus, the constraints defined in (7) can also be written as

$$\begin{aligned} \mathrm{Tap}^{\mathrm{up}}_{\alpha} &\le \mathrm{Tap}^{\mathrm{up}}_{\mathrm{limit}} \\ \mathrm{Tap}^{\mathrm{low}}_{\alpha} &\ge \mathrm{Tap}^{\mathrm{low}}_{\mathrm{limit}}. \end{aligned} \tag{11}$$

The *Tap Tail Expectation* is an alternative risk measure that takes into account the tail of probability distribution of variable Tap. For the variable Tap and with confidence level $\alpha \in [0,1]$, the Tap Tail Expectation is the mean of the tail distribution. If $F_{\mathrm{Tap}}(\mathrm{Tap}^{\mathrm{up}}_{\alpha}) < 1$, then there is a possibility of a VR operating above $\mathrm{Tap}^{\mathrm{up}}_{\alpha}$ value. Then the *Tap Tail Expectation* $E[\mathrm{Tail}^{\mathrm{up}}_{\alpha}(\mathrm{Tap})]$ is calculated as follows [30]:

$$\begin{aligned} E[\mathrm{Tail}^{\mathrm{up}}_{\alpha}(\mathrm{Tap})] = {} & \Psi_{\alpha}(\mathrm{Tap})\mathrm{Tap}^{\mathrm{up}}_{\alpha} \\ & + (1 - \Psi_{\alpha}(\mathrm{Tap}))E[\mathrm{Tap} | \mathrm{Tap} > \mathrm{Tap}^{\mathrm{up}}_{\alpha}] \end{aligned} \tag{12}$$

$$\Psi_{\alpha}(\mathrm{Tap}) = \frac{F_{\mathrm{Tap}}(\mathrm{Tap}^{\mathrm{up}}_{\alpha}) - \alpha}{1 - \alpha}. \tag{13}$$

Thus, it can be seen that *Tap Tail Expectation* the weighted average of $(\mathrm{Tap}^{\mathrm{up}}_{\alpha})$ and $E[\mathrm{Tap} | \mathrm{Tap} > \mathrm{Tap}^{\mathrm{up}}_{\alpha}]$. It should be noted that similarly for the lower limit of a VR $E[\mathrm{Tail}^{\mathrm{low}}_{\alpha}(\mathrm{Tap})]$ can be defined. The above *Tap Tail Expectation* indices can be

incorporated in the proposed CCO strategy by replacing the constraints in (7) by

$$E[\mathrm{Tail}_{\alpha}^{\mathrm{up}}(\mathrm{Tap})] \leq \epsilon_{\mathrm{Taptail}}^{\mathrm{up}}$$
$$E[\mathrm{Tail}_{\alpha}^{\mathrm{low}}(\mathrm{Tap})] \geq \epsilon_{\mathrm{Taptail}}^{\mathrm{low}}. \quad (14)$$

By selecting an appropriate value of $\epsilon_{\mathrm{Taptail}}^{\mathrm{up}}$, $\epsilon_{\mathrm{Taptail}}^{\mathrm{low}}$, DNOs can control the shape of the VR tail probability distribution. For instance, again consider that the permissible probability of the tap value being beyond $+11$ is 5%. DNOs desire the $\epsilon_{\mathrm{Taptail}}^{\mathrm{up}}$ to be $+12$. Then, constraint in (14) will not only try to have less than 5% probability above $+11$ but also will try to have expected value of the tail less than or equal to $+12$. This will avoid scenarios such as all the 5% operation of a VR at $+16$, which is possible with classical constraints (7). Thus, constraints defined in (14) will ensure an operational margin for a VR.

In order to achieve this, all voltage control equipments and PV inverter control features (e.g., reactive power injection and active power curtailment) need to be coordinated to achieve this. The effectiveness of modeling VR runaway in classical CCO and using the *Tap Tail Expectation* is demonstrated in the next section using a realistic distribution test system model.

V. Case Study

A. System Model

The U.K. generic distribution system (UKGDS), displayed in Fig. 7, is considered. The system is a 95-bus test system fed by the substation transformer equipped with an OLTC (33/11 kV) [31]. A base voltage of 11 kV and a base power of 100 kVA are assumed. There are two PV plants considered in the system each of 1 MW capacity. The PV inverter MVA capacity is overrated such that the plant is able to operate at 0.95 lead/lag pf during the peak active power injection. Practical irradiance measurements carried out on a 5-s time scale at Loughborough, England in the month of July 2012, are used. The base power considered is 100 kVA, i.e., a load of 100 kVA is equivalent to 1 p.u. The average value of peak solar generation is 7 p.u. while that of load is 18 p.u. PV generation forecast errors are modeled by a Gaussian distribution [32]. The PV generation forecast error pdfs are shown in Figs. 8 and 9. A correlation coefficient of 0.7 is considered between the two PV generators at bus 18 and bus 89. Correlation coefficient between PV and load is assumed -0.68 in morning and 0.21 in afternoon (after 12 noon) [33]. Load forecast errors are also modeled by a Gaussian distribution [16], [34]. The load forecast errors are shown in Figs. 10 and 11.

There are two VRs connected in the system, one between bus 54 and bus 75 (VR1), and the other between bus 24 and bus 23 (VR2). The OLTC and both VRs have an operational range $+16$ to -16. Timer controlled switched capacitors are widely used in European distribution networks [35]. Two banks of switched capacitors namely, C1 and C2, each of rating 200 kVAr at rated voltage (1 p.u.), are assumed to be installed at bus 52. Capacitor C1 is switched ON at 17:00 h and switched OFF at 3:00 h. Capacitor C2 is switched ON at 17:00 h and switched OFF at 8:00 h. The next section discusses various results obtained from this example.

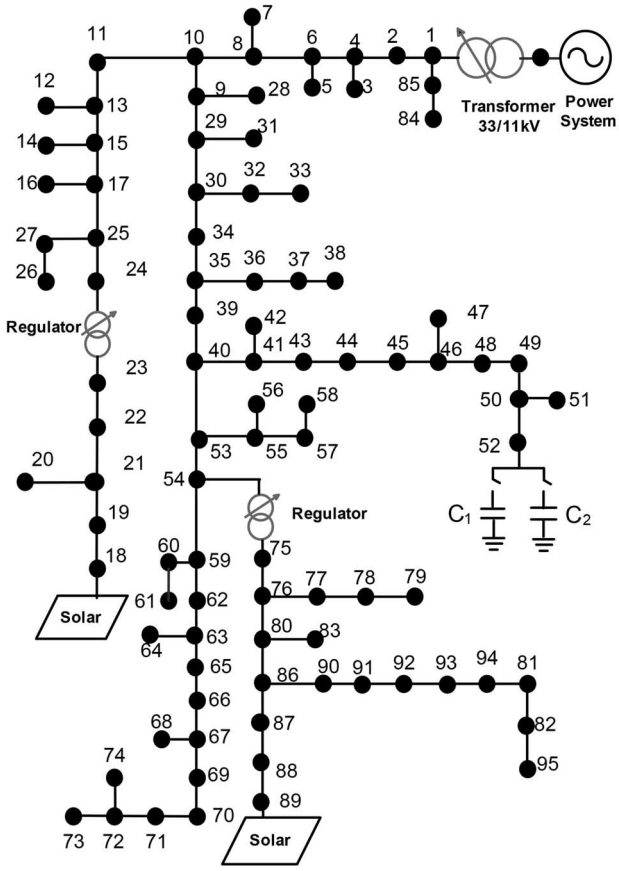

Fig. 7. UKGDS 95 bus test system.

B. Results

Three different cases are studied to evaluate the performance of the proposed strategy.

Case 1: Deterministic setpoint calculation.

Case 2: Classical CCO.

Case 3: CCO with *Tap Tail Expectation.*

For these three cases, first voltage control device setpoints are designed. Then using these setpoints, a PLF is calculated to evaluate the operational performance of the system. The upcoming sections discuss the detailed results and the performance comparison.

1) Case 1. Deterministic Setpoint Calculation: In this case, system voltage control is achieved by designing setpoints using a deterministic optimization strategy. This strategy ignores uncertainties associated with load and irradiance and assumes that day-ahead load and irradiance profiles are known accurately. Also, all the chance constraints are replaced by the deterministic constraints. The deterministic optimization is setup and a penalty function approach is utilized to avoid VR runaway as proposed in [11]. The coordinated operation of OLTC, VR, and PV plant is achieved and detailed voltage setpoint calculation is carried out as per the procedure explained in [11]. In reality, PV generation and load forecasts will have errors. These errors are

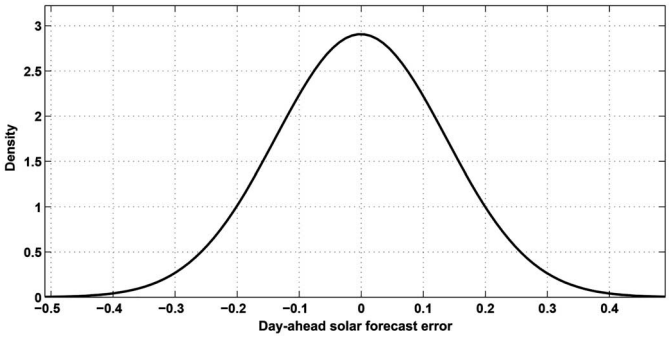

Fig. 8. PV generation day-ahead forecast error pdf.

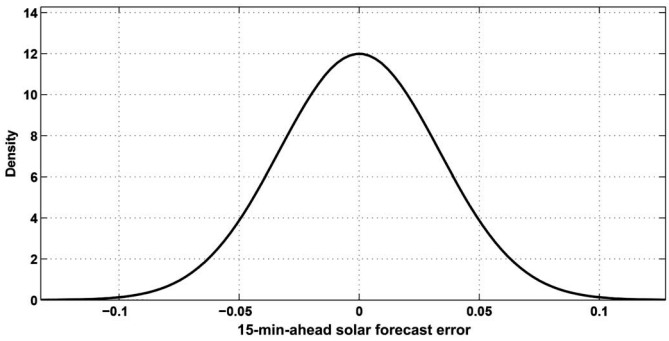

Fig. 9. PV generation 15-min-ahead forecast error pdf.

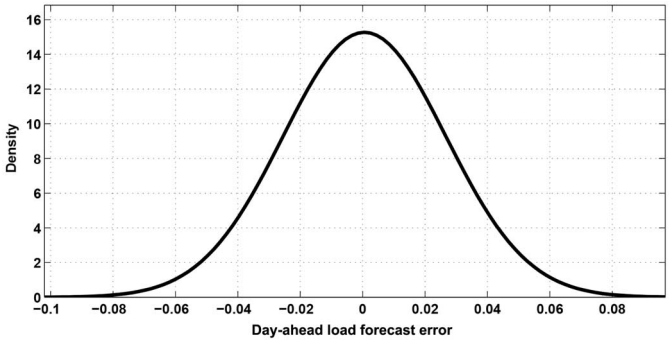

Fig. 10. UKGDS day-ahead load forecast error pdf.

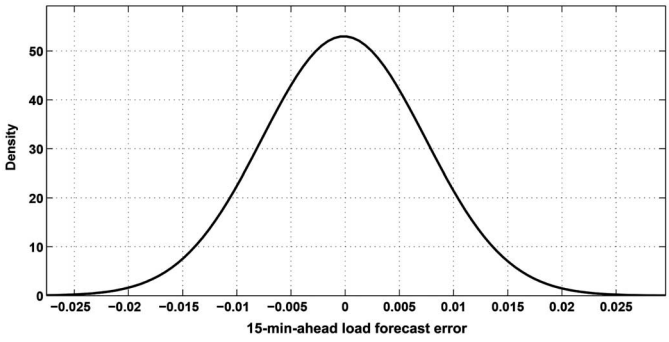

Fig. 11. UKGDS 15-min-ahead load forecast error pdf.

introduced and the PLF is run. The boxplots of the voltage magnitudes at various buses over a day are shown in Fig. 12. It can be observed that the probability of violating the voltage limits is zero. However, pdfs for both the VRs are shown in Fig. 13,

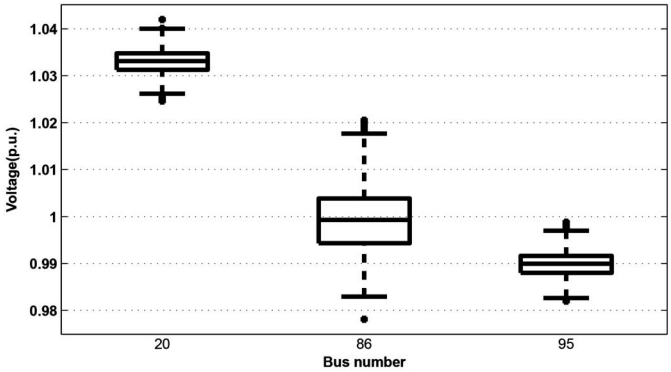

Fig. 12. Case 1: Boxplot of UKGDS bus voltages.

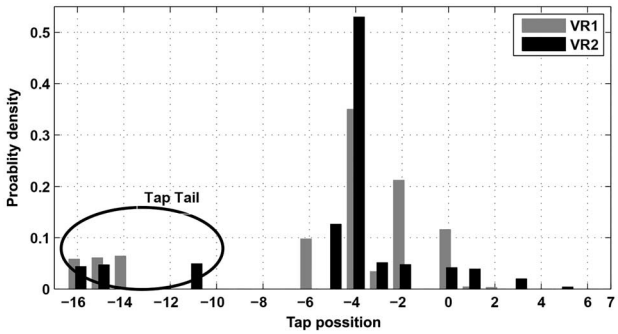

Fig. 13. Case 1 VR operation pdfs: unacceptable tail distribution.

from which it can be observed that the probability of operation at the tap position -16 (operational limit) for VR1 is 5.8% and for VR2 is 4.3%. Also, 18.33% of VR1 operation and 14% of VR2 operation happen in the tail region (Tap value below -10). This indicates a fairly small VR operational margin in these scenarios. This unsatisfactory operational performance of VRs is because setpoint calculation is without considering forecast errors. In order to alleviate this challenge, the following two cases evaluate the proposed CCO-based strategies.

2) Case 2. Classical CCO: In order to avoid VR runaway and maintain VR control margin, the classical CCO as described in Section II is used. To minimize the VR runaway probability, the constraints defined in (7) are considered. This exercise designates regions beyond Tap values of ± 10 of VR as *nonpreferred zones*. Ideally, the optimization should result in setpoints such that, the VR operation in the *nonpreferred zone* becomes a zero-probability event, or the nonpreferred zone Tap values should have very small probability. Hence, the setpoints should make the *nonpreferred zones* lie in the *tail* region of the VR Tap value pdf. In order to achieve this, the constraints in (7) are employed. A 5% violation probability is permissible beyond Tap values $+10$ and -10. Based on the operator's experience, an appropriate choice of violation probability and *nonpreferred zones* can be made to maintain a VR control margin. After defining these parameters, the classical CCO-based coordination is simulated. The resultant Tap pdfs for both VRs are shown in Fig. 14. The following observations can be made comparing "Case 1" in Fig. 13 and "Case 2" in Fig. 14. It can be observed that there is a reduction in the probability of VR operation in the nonpreferred zone beyond the Tap value

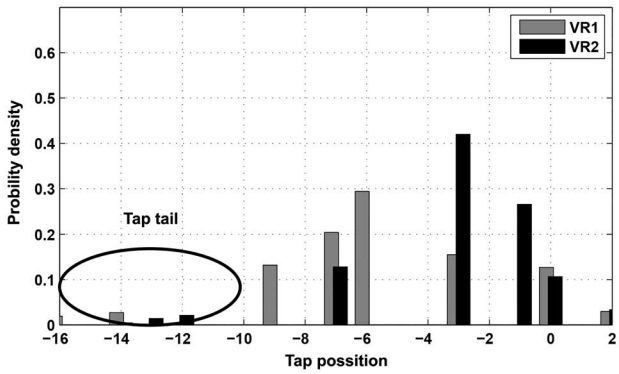

Fig. 14. Case 2. VR operation pdfs: reduction in nonpreferred zone probability.

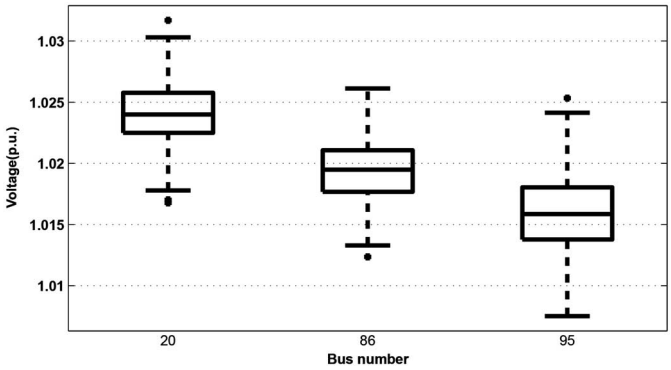

Fig. 15. Case 2: Boxplot of UKGDS bus voltages.

TABLE I
CASE 2: PV GENERATION VOLTAGE SETPOINTS (P.U.) FROM 11:00 A.M. TO 12:00 P.M.

Bus 89	1.025	1.015	1.02	1.02
Bus 18	1.03	1.025	1.025	1.02

± 10. The probability of the operation below -10 is less than 5%. Similar to the VR operation, the violation probability is defined for the voltage. Fig. 15 shows the boxplot of UKGDS bus voltage magnitudes. It can be observed that the voltage at the buses is maintained between $0.95 - 1.05$ p.u. The above classical CCO-based reactive power coordination is achieved with optimal PV generation setpoints. Optimal PV generation setpoints for bus 18 and bus 89 are shown in Table I. Thus, the formulation helps minimizing the VR runaway probability and maintains bus voltages within their prescribed limits.

3) Case 3. CCO With Tap Tail Expectation: Closer observation of Fig. 16 indicates the limitation of the classical CCO. There is still a small probability of VR operation at -16 (approximately 2%). This shows that the modeling of the violation probability as per (7), reduces the probability of operation beyond the Tap value -10 to a value below 5%. But in the 5% of the scenarios, there is no control at which position VR will operate. As can be observed in Fig. 16, this can very well be -16 indicating operation at the VR tap limit. Considering this limitation, the *Tap Tail Expectation* as defined in Section IV is used in the simulation.

Runaway related constraints are replaced by (14). The $\epsilon^{\mathrm{up}}_{\mathrm{Taptail}}$ and $\epsilon^{\mathrm{low}}_{\mathrm{Taptail}}$ parameter values are considered to be ± 12.

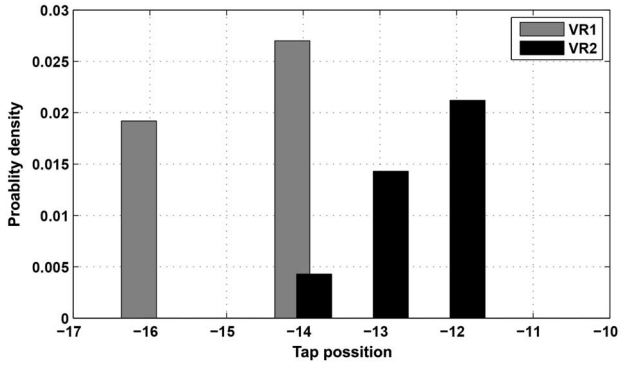

Fig. 16. Case 2: Lack of control over the shape of VR tail distribution.

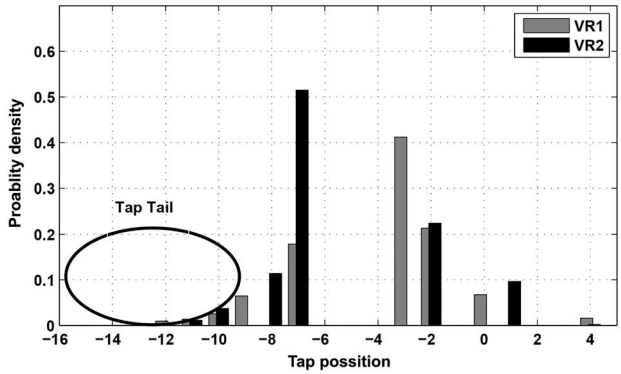

Fig. 17. Case 3 VR operation pdfs: satisfactory operational margin.

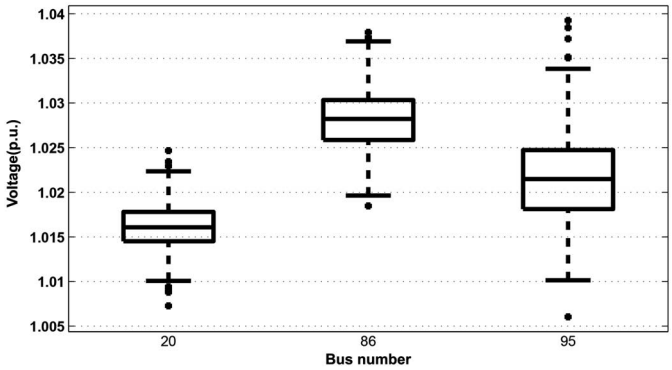

Fig. 18. Case 3: Boxplot of UKGDS bus voltages.

Fig. 17 shows the effectiveness of the *Tap Tail Expectation*. The probability of runaway is reduced further and the VR operational margin is improved. This is because the expected value of the Tap in the tail of the distribution is designed to be greater than -12. Therefore, defining constraints using the *Tap Tail Expectation* offers control over the tail region of Tap. In this study, the *Tap Tail Expectation* is defined only for VRs. The voltage optimization is carried out by defining the violation probability. The resultant boxplot curves of the UKGDS bus voltage magnitudes are shown in Fig. 18. The optimal PV generation set points for bus 18 and bus 89, for this case, are shown in Table II.

As discussed in Section II, other operational targets such as power loss minimization and tap operational counts minimization are also considered in "Case 2" and "Case 3." Table III

TABLE II
CASE 3: PV GENERATION VOLTAGE SETPOINTS (P.U.) FROM 11:00 A.M. TO 12:00 P.M.

Bus 89	1.035	1.025	1.025	1.03
Bus 18	1.015	1.02	1.025	1.02

TABLE III
UKGDS 95 BUS SYSTEM OPERATIONAL PERFORMANCE

Case	*E*(energy loss)	*E*(tap counts)
Case 1	2.65MWh	38
Case 2	2.44MWh	25
Case 3	2.53MWh	29

shows the expected values of power loss in the network and the tap counts for all the cases. Case 2 demonstrates the classical CCO-based approach and Case 3 demonstrates the Tap Tail Expectation-based method. Case 1 is a deterministic method, which ignores forecast errors. The methods demonstrated by Cases 2 and 3 alleviate the challenges related to energy loss and tap counts as compared to Case 1. In Case 2, power losses are reduced by 8% and tap counts are reduced by 34% as compared to Case 1. In Case 3, power losses are reduced by 4.5% and tap counts are reduced by 23.5% as compared to Case 1. Case 2 gives better performance than Case 3 for energy loss and tap counts. However, the tap tail expectation-based method (Case 3) helps the operator to predesign the VR control margin. The classical CCO-based approach (Case 2) can only have a control over the probability of VR operation near the limits, but it cannot control the VR operational margin. Thus, the proposed CCO-based reactive power coordination through classical and *Tap Tail Expectation* approaches are effective in improving the operational performance of the system such as network losses and the number of tap movements. The proposed approach successfully minimizes the CCO computational burden by choosing N representative samples based on (8). The algorithm is programmed in MATLAB and runs on a simple Pentium IV computer, 2.53 GHz with 12 GB RAM. For a day-ahead horizon planning, the solution is achieved in less than 15 min. Note this is just a onetime calculation aimed at calculating the OLTC setpoints for a day. Also, note that a day-ahead planning step can be completely omitted by operators as the algorithm also has a second stage, which considers shorter time interval and recalculates setpoints for PV inverter. Operators can consider only the second stage. In this case study, the second stage considers a 15-min-ahead time horizon. For a 15-min-ahead horizon, the solution is achieved on a simple Pentium IV computer, 2.53 GHz with 12 GB RAM in less than 2 min. If this algorithm is implemented using a higher performance computer (such as Intel I3, I5, or I7), the solution for a 15-min-ahead planning interval can be achieved in few seconds.

These case studies can be summarized as follows.

1) The state-of-the-art distribution system voltage regulation techniques do not consider forecast errors associated with PV generation and load. In previous techniques, the phenomenon of VR runaway is also not considered while calculating operational setpoints of regulating devices that control distribution feeder voltages.
2) The method considered in Case 1 is representative of the present day practice. The solution calculated using the methodology described in Case 1 does not hold true when forecast errors are considered. This can lead to suboptimal performance of distribution feeders. In Case 1, the power losses and tap operations are higher; additionally, the VR runaway phenomenon is not considered.
3) Considering these aspects, the authors propose two methods in this paper. These methods are demonstrated in Cases 2 and 3. Both methods successfully alleviate the limitations in Case 1 (present day practice).

VI. CONCLUSION

The conventional framework to achieve the distribution voltage control in the presence of PV generation does not consider inevitable forecasting errors. It is essential to mitigate the operational risks such as overvoltage, excessive tap counts, and VR Runaway, in the presence of PV and load forecast errors. This is achieved via a stochastic optimization-based voltage control strategy. Two variants of CCO are proposed to minimize the risk of VR runaway. A classical CCO considers the runaway phenomenon by modeling the violation probability and by defining Tap *nonpreferred zones*. An improvement to this approach is proposed by defining the *Tap Tail Expectation* index as part of the CCO constraints. The problem is solved using a sample selection-based approach. The simulation study carried out using a realistic distribution system model shows satisfactory results. It is observed that both CCO-based approaches are able to reasonably minimize the probability of VR runaway. However, the classical CCO-based approach does not control the shape of the tail probability distribution. In the classical CCO approach, the expected value of the tail can lie near the VR operational limit. The *Tap Tail Expectation*-based approach offers control over the tail region of the Tap and offers a robust operational margin for VR. Both these approaches also minimize the power loss and excessive tap counts. These proposed CCO-based strategies will be useful to DNOs to ensure efficient and risk averse network operation in the presence of PV generations.

ACKNOWLEDGMENT

The authors would like to thank Dr. T. Betts from Loughborough University, U.K. for solar irradiance data.

REFERENCES

[1] G. Masson, M. Latour, M. Rekinger, I. Theologitis, and M. Papoutsi, "Global market outlook for photovoltaics 2013-2017," Technical Paper, Eur. Photovoltaic Energy Assoc. (EPIA), Mar. 2013 [Online]. Available: http://www.epia.org/

[2] J. Appen, M. Braun, T. Stetz, K. Diwold, and D. Geibel, "Time in the sun: The challenge of high PV penetration in the german electric grid," *IEEE Power Energy Mag.*, vol. 11, no. 2, pp. 55–64, Mar. 2013.

[3] C. Winneker, Ed. (2012, Sep.) *Connecting the Sun Solar Photovoltaics on the Road to Large Scale Integration* [Online]. Available: http://www.epia.org/

[4] A. G. Madureira and J. A. P. Lopes, "Coordinated voltage support in distribution networks with distributed generation and microgrids," *IET Renew. Power Gener.*, vol. 3, no. 4, pp. 439–454, Dec. 2009.

[5] T. Basso, J. Hambrick, and D. DeBlasio, "Update and review of ieee p2030 smart grid interoperability and IEEE 1547 interconnection standards," in *Proc. IEEE PES Innovative Smart Grid Technol. (ISGT)*, Washington, DC, USA, Jan. 2012, pp. 1–7.
[6] A. Malekpour and A. Pahwa, "Reactive power and voltage control in distribution systems with photovoltaic generation," in *Proc. North Amer. Power Symp. (NAPS)*, Sep. 2012, pp. 1–6.
[7] R. A. Walling and K. Clark, "Grid support functions implemented in utility-scale PV systems," in *Proc. IEEE PES Transmiss. Distrib. Conf. Expo.*, New Orleans, LA, USA, Apr. 2010, pp. 1–5.
[8] Federal Ministry for the Environment, Nature Conservation and Nuclear Safety (BMU), Germany, "Renewable energy sources act-EEG," Jan. 2012, Consolidated (non-binding) version of the Act applicable as at Jan. 1, 2012 [Online]. Available: http://www.bmub.bund.de/
[9] B. Seal. (2010, May) *Standard Language Protocols for Photovoltaics and Storage Grid Integration Developing a Common Method for Communicating With Inverter-Based Systems* [Online]. Available: http://www.smartgridnews.com/
[10] M. McGranaghan, T. Ortmeyer, D. Crudele, T. Key, J. Smith, and P. Barker, "Renewable systems interconnection study advanced grid planning and operations," Sandia National Lab., Albuquerque, NM, USA, Feb. 2008.
[11] Y. Agalgaonkar, B. C. Pal, and R. A. Jabr, "Distribution voltage control considering the impact of PV generation on tap changers and autonomous regulators," *IEEE Trans. Power Syst.*, vol. 29, no. 1, pp. 182–192, Jan. 2014.
[12] T. Senjyu, Y. Miyazato, A. Yona, N. Urasaki, and T. Funabashi, "Optimal distribution voltage control and coordination with distributed generation," *IEEE Trans. Power Del.*, vol. 23, no. 2, pp. 1236–1242, Apr. 2008.
[13] F. A. Viawan and D. Karlsson, "Combined local and remote voltage and reactive power control in the presence of induction machine distributed generation," *IEEE Trans. Power Syst.*, vol. 22, no. 4, pp. 2003–2012, Nov. 2007.
[14] S. Paudyal, C. A. Canizares, and K. Bhattacharya, "Optimal operation of distribution feeders in smart grids," *IEEE Trans. Ind. Electron.*, vol. 58, no. 10, pp. 4495–4503, Oct. 2011.
[15] W. Glassley, J. Kleissl, H. Shiu, J. Huang, G. Braun, and R. Holland, "Final report on current state of the art in solar forecasting," California Renewable Energy Forecasting, Resource Data and Mapping, California Renewable Energy Collaborative, Tech. Rep. CEC-500-2014-026, 2012.
[16] B. M. Hodge, D. Lew, and M. Milligan, "nrel/cp550057340 short-term load forecasting error distributions and implications for renewable integration studies," in *Proc. IEEE Green Technol. Conf.*, Denver, CO, USA, Apr. 2013, pp. 1–8.
[17] M. Fan, V. Vittal, G. Heydt, and R. Ayyanar, "Probabilistic power flow studies for transmission systems with photovoltaic generation using cumulants," *IEEE Trans. Power Syst.*, vol. 27, no. 4, pp. 1–12, Nov. 2012.
[18] M. Fan, V. Vittal, G. Heydt, and R. Ayyanar, "Probabilistic power flow analysis with generation dispatch including photovoltaic resources," *IEEE Trans. Power Syst.*, vol. 28, no. 3, pp. 1–9, May 2013.
[19] Y. Kim, S. Ahn, P. Hwang, G. Pyo, and S. Moon, "Coordinated control of a DG and voltage control devices using a dynamic programming algorithm," *IEEE Trans. Power Syst.*, vol. 28, no. 1, pp. 42–51, Feb. 2013.
[20] T. Karakatsanis and N. Hatziargyriou, "Probabilistic constrained load flow based on sensitivity analysis," *IEEE Trans. Power Syst.*, vol. 9, no. 4, pp. 1853–1860, Nov. 1994.
[21] N. Hatziargyriou, T. Karakatsanis, and M. Papadopoulos, "Probabilistic load flow in distribution systems containing dispersed wind power generation," *IEEE Trans. Power Syst.*, vol. 8, no. 1, pp. 159–165, Feb. 1993.
[22] H. Zechun, W. Xifan, and G. Taylor, "Stochastic optimal reactive power dispatch: Formulation and solution method," *Int. J. Elect. Power Energy Syst.*, vol. 32, no. 6, pp. 615–621, Jul. 2010.
[23] P. Chen, S. Pierluigi, B. Jensen, and Z. Chen, "Stochastic optimization of wind turbine power factor using stochastic model of wind power," *IEEE Trans. Sustain. Energy*, vol. 1, no. 1, pp. 19–29, Apr. 2010.
[24] C. L. Masters, "Voltage rise: The big issue when connecting embedded generation to long 11 kV overhead lines," *Power Eng. J.*, vol. 16, no. 1, pp. 5–12, Feb. 2002.
[25] P. A. N. Garcia, J. L. R. Pereira, and S. Carneiro Jr, V. M. daCosta, and N. Martins, "Three-phase power flow calculations using the current injection method," *IEEE Trans. Power Syst.*, vol. 15, no. 2, pp. 508–514, May 2000.
[26] P. A. N. Garcia, J. L. R. Pereira, and S. Carneiro Jr, "Voltage control devices models for distribution power flow analysis," *IEEE Trans. Power Syst.*, vol. 16, no. 4, pp. 586–594, Nov. 2001.
[27] W. H. Kersting, Distribution System Modeling and Analysis. Boca Raton, FL, USA: CRC Press, 2002.
[28] G. Calafiore and M. Campi, "Uncertain convex programs: Randomized solutions and confidence levels," *Math. Programm.*, vol. 102, no. 1, pp. 25–46, Jan. 2005.
[29] I. Roytelman, B. Wee, and R. Lugtu, "Volt/Var control algorithm for modern distribution management system," *IEEE Trans. Power Syst.*, vol. 10, no. 3, pp. 1454–1460, Aug. 1995.
[30] S. Sarykalin, G. Serraino, and S. Uryasev, "Value-at-risk vs. conditional value-at-risk in risk management and optimization," in Tutorials in Operations Research. Hanover, MD, USA: INFORMS, 2008.
[31] R. Singh, B. C. Pal, and R. A. Jabr, "Distribution system state estimation through Gaussian mixture model of the load as pseudo-measurement," *IET Gener. Transmiss. Distrib.*, vol. 4, no. 1, pp. 50–59, Jan. 2010.
[32] C. Breuer, C. Engelhardt, and A. Moser, "Expectation-based reserve capacity dimensioning in power systems with an increasing intermittent feed-in," in *Proc. 10th Int. Conf. Eur. Energy Market (EEM)*, Stockholm, Sweden, May 2013, pp. 1–7.
[33] E. Troster and J. Schmidt, "Evaluating the impact of PV module orientation on grid operation," in *Proc. 2nd Int. Workshop Integr. Solar Power Power Syst.*, Lisbon, Portugal, 2012, pp. 253–258.
[34] B. Hodge *et al.*, "A comparison of wind power and load forecasting error distributions," *Proc. World Renew. Energy Forum*, 2012, pp. 1–8.
[35] F. A. Viawan and D. Karlsson, "Voltage and reactive power control in systems with synchronous machine-based distributed generation," *IEEE Trans. Power Del.*, vol. 23, no. 2, pp. 1079–1087, Apr. 2008.

Yashodhan P. Agalgaonkar (S'11) received the M.Sc. degree in electrical power engineering from Chalmers University of Technology, Gothenburg, Sweden, in 2006, and the Ph.D. degree in electrical engineering from the Imperial College London, London, U.K., in 2014.

He was a Postdoctoral Researcher at Imperial College London until recently. From 2006 to 2010, he was with Crompton Greaves, Aurangabad, India and with Converteam (now GE Energy), Chennai, India and Berlin, Germany as a Research Engineer. This work was carried out during the period at the Imperial College London, London, U.K. Presently, he is Scientist and Engineer with Pacific Northwest National Laboratory, Richland, WA, USA.

Bikash C. Pal (M'00–SM'02–F'13) received the B.E.E. (Hons.) degree from Jadavpur University, Calcutta, India, the M.E. degree from the Indian Institute of Science, Bangalore, India, and the Ph.D. degree from the Imperial College London, London, U.K, in 1990, 1992, and 1999, respectively, all in electrical engineering.

Currently, he is a Professor with the Department of Electrical and Electronic Engineering, Imperial College London. His research interests include state estimation, power system dynamics, and flexible ac transmission system controllers.

Rabih A. Jabr (M'02–SM'09) received the B.E. degree (with high distinction) from the American University of Beirut, Beirut, Lebanon, in 1997, and the Ph.D. degree from the Imperial College London, London, U.K., in 2000, both in electrical engineering.

Currently, he is a Professor with the Department of Electrical and Computer Engineering, American University of Beirut, Beirut, Lebanon. His research interests include mathematical optimization techniques and power system analysis and computing.